Supporting Information

Improved Stability and Photoluminescence Yield of Mn^{2+}-Doped $CH_3NH_3PbCl_3$ Perovskite Nanocrystals

Xianli Li[1,2,†], Yan Guo[1,2,†] and Binbin Luo[1,2,]*

a Department of Chemistry, Shantou University, Guangdong 515063, P. R. China

b Department of Chemistry and Key Laboratory for Preparation and Application of Ordered Structural Materials of Guangdong Province, Shantou University, Guangdong 515063, P. R. China

†: Contributed equally to this work

Table S1. Elemental analysis of $CH_3NH_3Pb_xMn_{1-x}Cl_3$ PNCs passivated with APTES under different doping concentration using ICP-AES.

Nominal concentration ($C_{Mn}/C_{Mn}+C_{Pb}$)	25 at. %	50 at. %	75 at. %	90 at. %
Detected concentration ($C_{Mn}/C_{Mn}+C_{Pb}$)	10.1 at. %	14.8 at. %	30.0 at. %	59.1 at. %

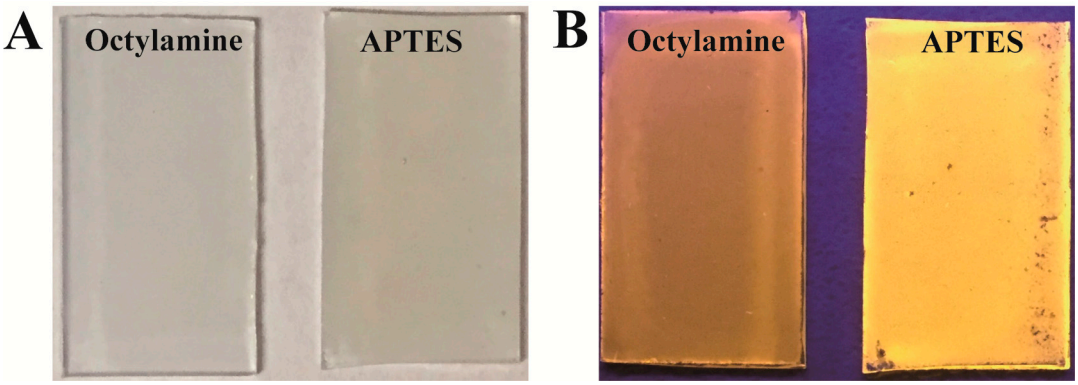

Figure S1. Photographs of 50 at. % Mn-doped $CH_3NH_3PbCl_3$ PNCs passivated with octylamine (left) and APTES (right) under room light (A) and 365 nm UV light (B).

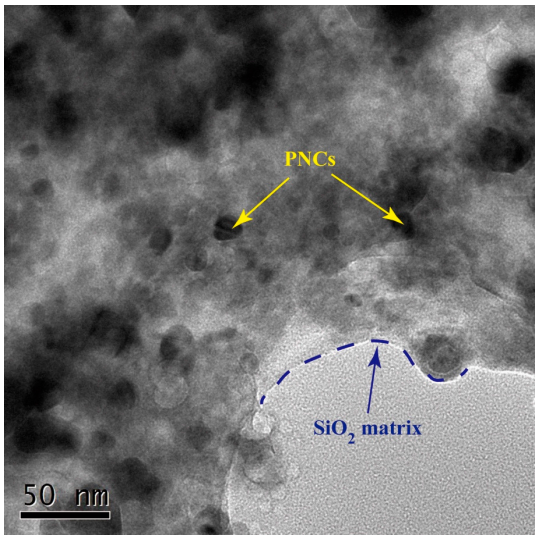

Figure S2. TEM image of $CH_3NH_3PbCl_3$ PNCs passivated with APTES.

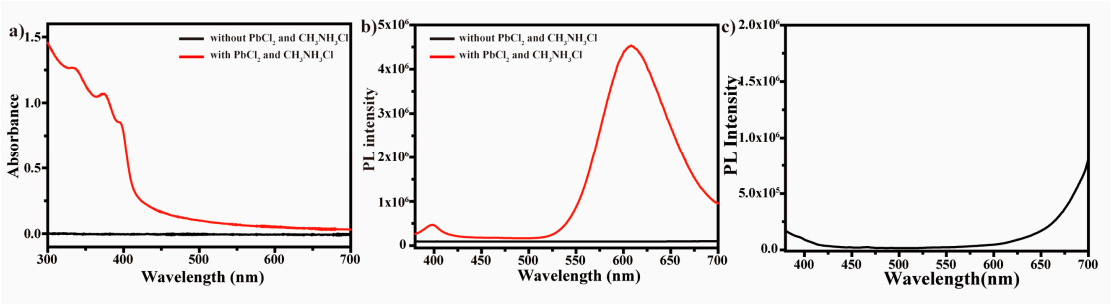

Figure S3. (a) Absorption and (b) PL spectra of solutions prepared using $MnCl_2$ and APTES precursors (black line), and using $MnCl_2$, APTES, $PbCl_2$ and CH_3NH_3Cl precursors (red line). (c) PL spectra of $MnCl_2$ (λ_{ex} = 360 nm).

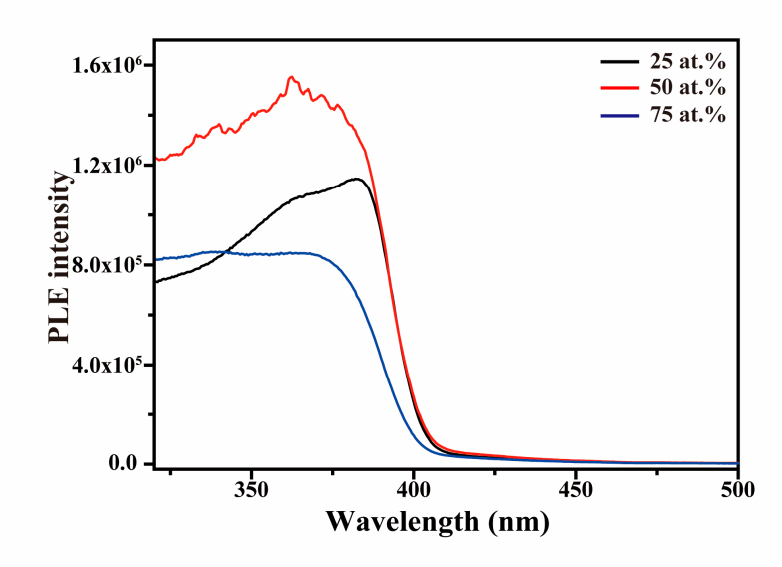

Figure S4. PLE spectra of Mn doped $CH_3NH_3PbCl_3$ PNCs with different doping concentration (λ_{em} = 610 nm).

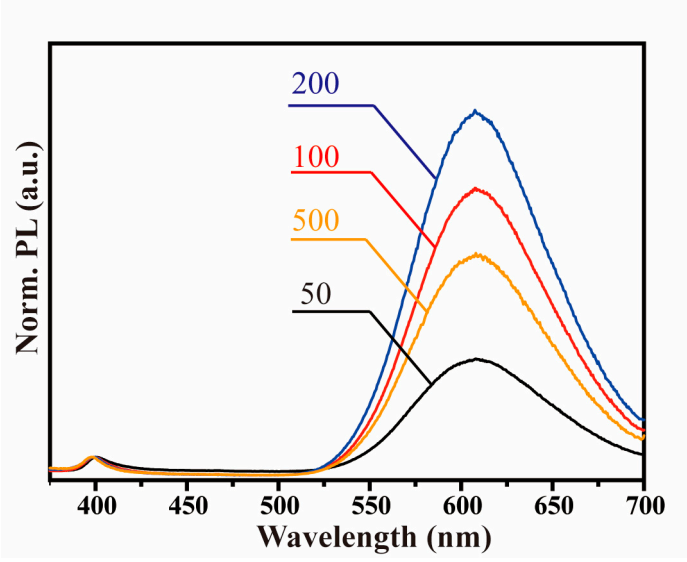

Figure S5. PL spectra of 50 at. % Mn-doped $CH_3NH_3PbCl_3$ PNCs solutions with different toluene/precursor volume ratios.

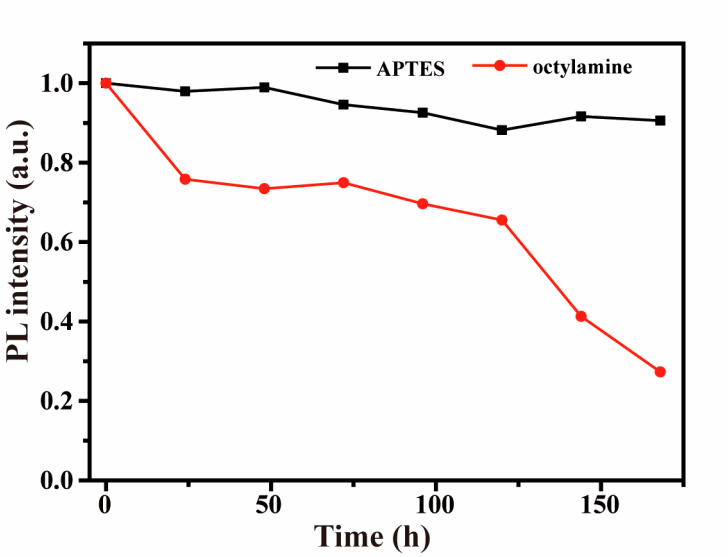

Figure S6. Air stability test of Mn-doped $CH_3NH_3PbCl_3$ PNCs passivated with octylamine and APTES.